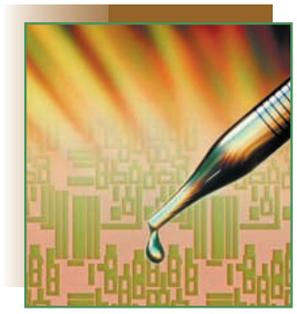

Microdevices for Dielectrophoretic Flow-Through Cell Separation

Comparing Experiments with Numerical Simulation for a Novel System that Separates and Fractionates Particles from a Fluid Stream

DAVID HOLMES, NICOLAS G. GREEN, AND HYWEL MORGAN

Many research groups have developed dielectrophoretic (DEP)-based separation systems for a wide range of particle types, including cells, bacteria, viruses and proteins [1]–[10]. Simple two-dimensional (2-D) spatial separation of a binary mixture of particles on a microelectrode array is relatively easy to demonstrate; however, the implementation of a practical flow-through separation system is rather more difficult and a range of continuous or bulk separation strategies have been devised. One type of DEP separator works by attracting particles out of a suspending medium by positive DEP. The medium flows over an electrode array, which is part of a flow-through chamber as shown in Figure 1. The frequency applied to the electrodes is chosen so that the cells of interest are attracted to the electrodes by positive DEP, and all the other cells experience negative DEP and are eluted from the device. Provided the flow velocity is not too high, the required particles remain trapped on the electrodes and can be released for postprocessing by switching off the field.

The separation chamber can be formed using a microelectrode array, for example, an interdigitated electrode, that generates a DEP force that is maximum at the surface and rapidly decreases (exponentially) into the chamber center. The simple device shown in Figure 1 has a number of practical problems; for example, the cells enter the chamber randomly distributed in the fluid carrier and therefore move at different velocities and experience the positive DEP force from the electrodes for different lengths of time. This leads to a completely random distribution of cells on the collection electrode even from a homogeneous population. Also, owing to the exponential profile of the DEP force, particles furthest from the electrodes often transit the device without being influenced by the DEP force and may not be captured. We have therefore developed a new type of DEP separator that consists of two microelectrode arrays integrated into a single device, as shown in Figure 2 [11], [12]. The first part of the device uses negative DEP to force a random distribution of particles entering the device into a well-defined sheet positioned midway between the upper and lower channel walls. This ensures that all particles enter the separation device at the same height, thereby eliminating any error in the collection point in the second array due to the exponential nature of the dielectrophoretic force.

The sheet of particles then enters the second separation electrode array, which is energized with a frequency such that the required subpopulation of particles is attracted to the electrode surface. Using this method, different subpopulations will collect on the second electrode array in clearly defined bands depending on their properties. This device can therefore also be used as a cell or particle fractionation device.

Another major problem with DEP-based separation systems is nonspecific adhesion of unwanted cells onto the collecting electrodes. Prefocusing the particles eliminates contact between the cells and the electrodes or the glass through sedimentation and therefore prevents adhesion.

In this article, we report on the numerical simulation of particle trajectories in this device and compare the simulations with experiments on the dielectrophoretic separation of white blood cells. Possible application of this DEP-separation device might be the separation of live from dead cells, the retrieval of small numbers of particles from a fluid containing debris, or the isolation of rare cells from a large population of unwanted particles with minimum contamination.

Materials

The separation devices were fabricated from two glass microscope slides bonded together with a spacer. Electrode arrays 10-mm wide and 20-mm long were patterned using standard photolithography and wet etching techniques. The spacer between the top and the bottom electrode was defined using SU8 photoepoxy of thickness 110 μm. The top and bottom halves were aligned and bonded using UV curable glue. Inlet and outlet holes were drilled prior to gluing the lid. As shown in Figure 2, two different electrode arrays were used. Both arrays were designed to have electrodes of equal width and gap = 40 μm, but in practice typical dimensions were an electrode gap = 44 μm and an electrode width = 36 μm. Particles flowing in the channel were observed using an epifluorescence microscope and images were recorded using a CCD camera captured directly to a PC. The two electrode arrays are driven by independent single-phase ac potential signals in the range of 1 kHz–20 MHz, 0–20 V.

Cell Preparation

The THP-1 cell line (human monocytic leukemia cells) was

 0739-5175/03/$17.00©2003IEEE

A microdevice was constructed from two consecutive arrays of microelectrodes, one to focus the particles into a sheet and the second to separate them using a combination of positive and negative DEP.

grown in culture from an initial sample of cells obtained from a continuous culture kept by Dr A. Gracie at Glasgow Royal Infirmary. The cells were maintained in culture media (500 ml of RPMI-1640 (25 mM Hepes and $NaHCO_3$) supplemented with, 5 ml L-glutamine, 5 ml Penicillin/Streptomycin, 2 ml Fungizone and 10% fetal calf serum) at 37°C in a 5% CO_2 atmosphere. THP-1 cells were harvested just prior to experiments and resuspended in low conductivity, dielectrophoretic separation media at cell concentrations of $\sim 10^5$ cells/ml.

The dielectrophoretic separation medium consisted of dH_2O with 9% sucrose (w/v), 3.5% Ficoll400 (w/v), 0.1% glucose (w/v), 0.8% BSA (w/v), and 1mM EDTA. Ficoll400 was added to increase the density of the separation medium and eliminate the effects of cell sedimentation. The addition of Ficoll increases the density of a suspension media in approximately the same way as sucrose. However, due to its large size the Ficoll molecule (MW = 400,000) does not permeate through the cell membrane, and as such its addition does not alter the osmotic balance of the media. The permittivity of the medium is also unchanged by the addition of the neutral Ficoll molecule. The pH and conductivity were adjusted by the addition of small amounts of mono- or dibasic phosphate buffer. The capacitance of the cells was determined from cross-over measurements [10], [13] and found to be 17.7 ± 2.7 mF/m^2 with a mean cell radius of 6.4 um ± 1 μm [14].

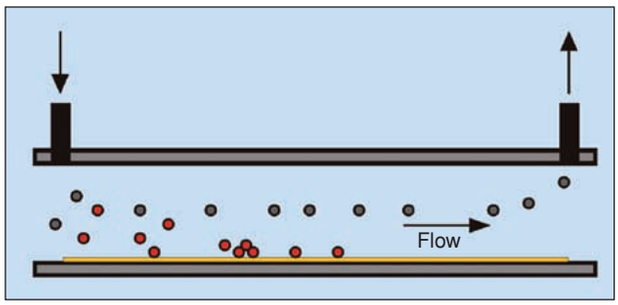

Fig. 1. Schematic diagram of one mechanism of dielectrophoretic separation over a long array of interdigitated electrodes. Particles flow through the device, some collecting on the electrodes through positive DEP, while others are repelled into the middle of the channel and are removed by the fluid flow.

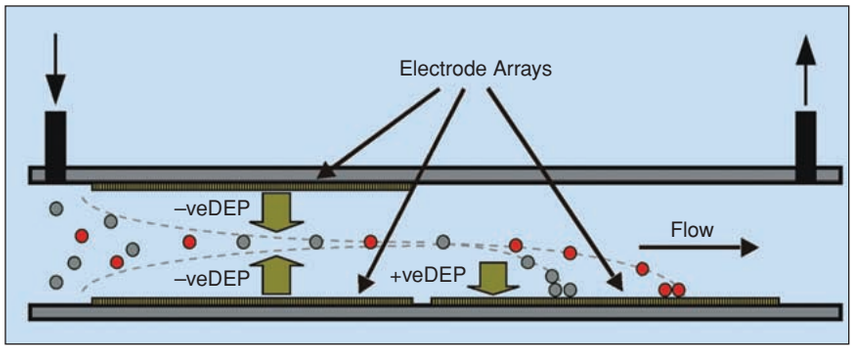

Fig. 2. Schematic diagram of the dielectrophoretic separator. The first section of the device has two interdigitated electrode arrays at top and bottom of the channel, which focus the particles into the center of the channel by negative DEP. The second section contains a single electrode array, which differentially pulls the focused particles from the fluid flow by positive DEP, separating them into distinct bands.

Theory and Simulation

Ignoring Brownian motion, the deterministic forces acting on a particle can be divided into the horizontal and vertical components. This is summarized in Figure 3, together with a diagram illustrating the parabolic nature of the fluid velocity that occurs for low Reynolds numbers in a microchannel. The vertical component of the DEP force can act either with or against the buoyancy force (generally cells are more dense than the suspending medium). The steady-state equation of motion in this vertical (or y) axis is therefore:

$$\mathbf{v}_y = \frac{\mathbf{F}_{DEP,y} + \mathbf{F}_{Buoyancy}}{f} \qquad (1)$$

where f is the friction factor, which for a spherical particle is $6\pi\eta a$, with a = particle radius and η the viscosity of the fluid.

In the horizontal plane (x-direction), the force acting on the particle is predominantly the Stokes force due to the movement of the fluid and any x-component of the DEP force, which must be taken into account when particles are close to the electrode. In a narrow channel the fluid adopts the parabolic or Pousseille flow profile with a velocity given by

$$\mathbf{u}_x = \frac{1}{2\eta}\frac{p}{l}(d^2 - y^2) \qquad (2)$$

where d is the half height of the channel, and p/l is the pressure drop across the length of the channel. The equation governing the particle velocity in the x-direction is therefore

$$\mathbf{v}_x = \mathbf{u}_x + \frac{\mathbf{F}_{DEP,x}}{f}. \qquad (3)$$

For comparison of numerical values with the experiment, it is convenient to calculate the volume flow rate through the device, which is derived by integrating (2) and is given by

At a flow rate of 1 ml/hour, experiments showed that THP-1 cells were captured on the electrode array and that the banding of cells was consistent with a full numerical simulation of the system.

$$Q = \frac{wh^3}{12\eta}\frac{p}{l} \tag{4}$$

Here w is the width and h the height of the device (*n.b.* $h = 2d$).

The time-averaged DEP force is given by [10], [15]:

$$\mathbf{F}_{DEP} = \pi a^3 \varepsilon_m \mathrm{Re}\{f_{CM}\}\nabla|\mathbf{E}|^2 \tag{5}$$

where $\mathbf{E}$ is the peak electric field of angular frequency ω, a the particle radius, and Re{ } indicates the real part. The factor f_{CM} is a measure of the effective polarizability of the particle (the Clausius-Mossotti factor) given by:

$$f_{CM} = \frac{\varepsilon_p^* - \varepsilon_m^*}{\varepsilon_p^* + 2\varepsilon_m^*} \tag{6}$$

where ε_p^* and ε_m^* are the complex permittivities of the particle and the medium, respectively, defined in general as $\varepsilon^* = \varepsilon - j\frac{\sigma}{\omega}$, where $j^2 = -1$, ε is the permittivity and σ is the conductivity of the dielectric. The Clausius-Mossotti factor indicates the relative magnitude and direction of the force experienced by a cell.

Equation (5) shows that the DEP force is, among other things, a function of the electric field magnitude and geometry $\nabla|\mathbf{E}|^2$ so that in order to simulate particle trajectories the spatial variation of $\nabla|\mathbf{E}|^2$ must be known. For the simulations presented in this work, the electric field from an array of interdigitated micro-electrodes was determined using two methods; an analytical approximation to the field and a finite-element numerical analysis [16]–[18]. Using (1) and (3) together with the appropriate expressions for the DEP force and sedimentation force, typical particle trajectories can be calculated.

Electric Field Calculation

Analytical Approximation

The full closed-form expression for the electric field gradient for the interdigitated electrode array is given in [16], [17]. This expression is derived from the infinite Fourier series for the potential from an infinite array of interdigitated electrodes assuming that the gap and electrode width are the same. In the expression for the analytical field, the voltage on one electrode, V_o is equal to one half of the amplitude of the potential difference applied to the electrodes. In this analytical solution, the boundary condition between the electrodes is approximated to a linear change in potential, which is not an accurate representation of the physical system. The analytical solution therefore underestimates the field and the DEP force by 13% when compared with a numerical solution with more representative boundary conditions [18]. Other approximate solutions have been derived that give a better degree of approximation [19], [20]; however, these series solutions are rather involved and more computationally expensive in the calculation of particle trajectories.

Numerical Solution

The electric field was calculated for two cases, one with the electrode gap and width set to 40 μm and another with the electrodes set equal to the fabricated devices with electrode width = 36 μ m and interelectrode gap = 44 μm. The simulations were performed by numerical calculation of Laplace's equation using the finite element method, details of which can be found in previous publications [10], [18].

Figure 4 shows a vector plot of the DEP force (proportional to $\nabla|\mathbf{E}|^2$) for the interdigitated electrode array, illustrating how the DEP force directs particles to the electrode edges (under positive DEP). Also shown is a plot of the $\log_{10}$(magnitude). The maximum value of the magnitude is close to the electrode edges. The plot shows the force vectors, indicating how the magnitude of the force decreases with distance from the electrode surface with an approximate decay length of the order of the electrode width [16].

Simulation of Particle Trajectory

Particle trajectories were calculated using an algorithm written in MATLAB using linear step integration of (1) and (3). This method calculates the position of a particle in space based on a velocity calculated for a small finite time step, which was typically 1 μs.

Experimental Results

Figure 5 shows a series of images taken during the collection of THP-1 cells onto the electrode array. These cells were

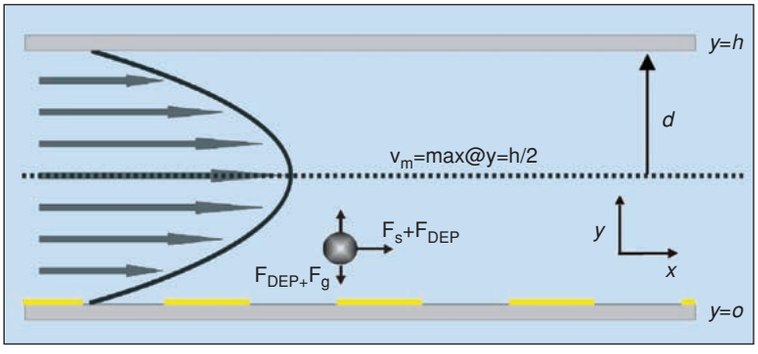

Fig. 3. Schematic diagram of the device, showing the different physical phenomena and the resulting forces on the particle.

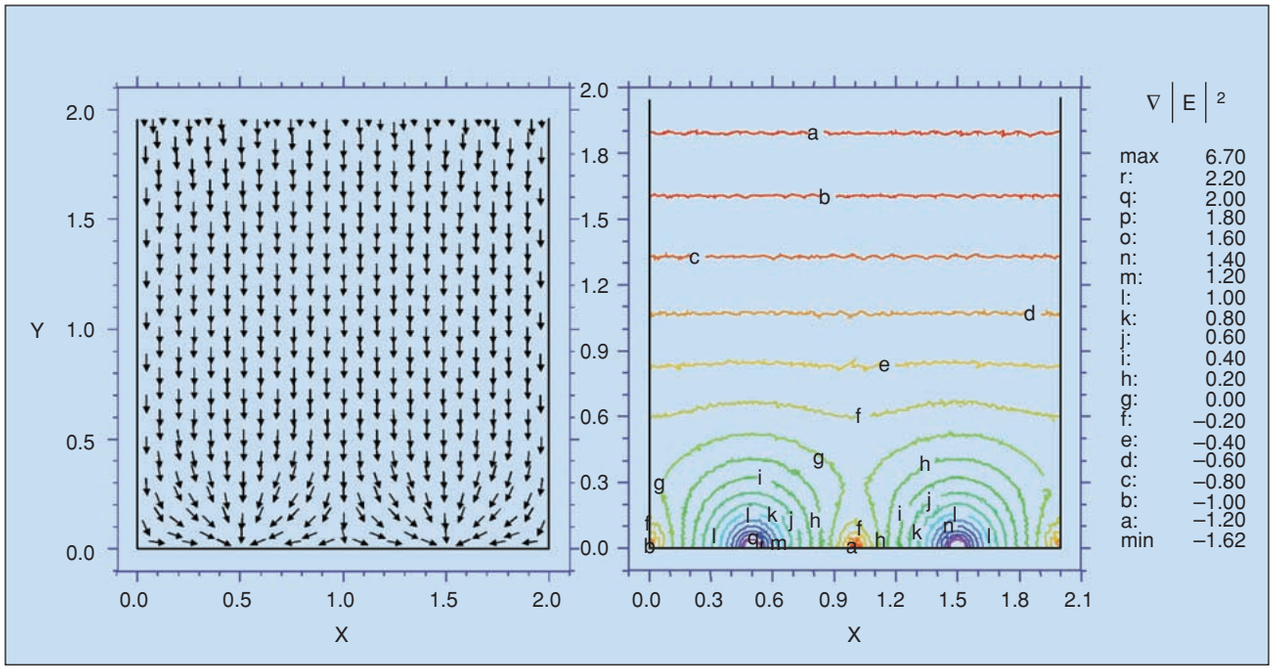

Fig. 4. Plot of the dimensionless numerical solution of the field-related term in the dielectrophoretic force expression. The arrow plot shows the direction of the vector and the contour plot shows the magnitude of the vector, with the $\log_{10}$ scale on the right. The electrodes are from 0 to 0.5 and from 1.5 to 2, with the vector pointing straight downwards above $y = \sim 0.5$ and then toward the electrode edges below this height. The magnitude also increases rapidly toward the edges.

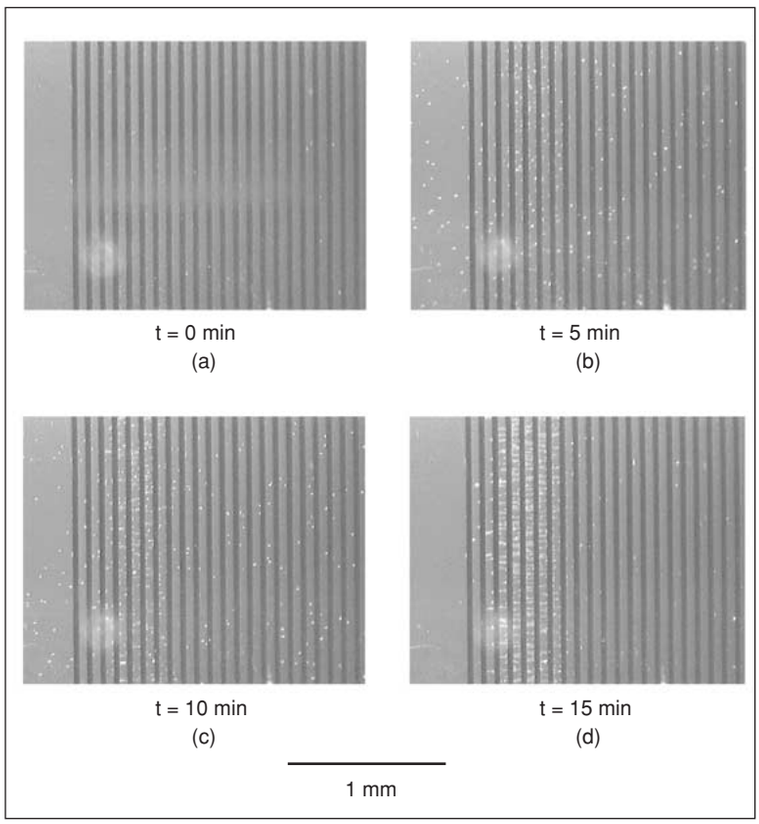

Fig. 5. A series of photographs of the collection of THP-1 cells onto an electrode array with gap = 44 μm and electrode width = 36 μm. The applied voltage was V_o = 3 V at a frequency of 150 kHz, the flow rate was 1 ml/hour, and the cell number density was 10^5 ml^{-1}.

processed with an electrode array of gap = 44 μm and a width of 36 μm, with $V_o = 3$ V at a frequency of 150 kHz. The flow rate was 1 ml per hour and the cell number density was 10^5 ml^{-1}.

Figure 5(a) show the electrode array at $t = 0$, with the end of the focusing array off to the left-hand side After 10 min a large number of cells have collected over the first few electrodes, with very few adhering anywhere else. The final image shows the electrode array at the end of the sample run (after 15 min), followed by 10 min of flushing the device with cell-free media. The series of images clearly shows that the cells collect in a well-defined band near the beginning of the electrode array. From the figure, the mean position of the band along the electrode array can be estimated to be approximately 400 μm with a width of approximately $\pm$150 μm.

The trajectories and ultimate position of the THP-1 cells on the electrodes were simulated using the procedure outlined above. The following experimental conditions were used for both simulation and experiment: suspending medium conductivity 26.3 mS m^{-1} (giving a Clausius-Mossotti factor of 0.623 at a frequency of 150 kHz); chamber width = 8 mm; volume flow rate = 1 ml/hour; differential density $\Delta\rho = 10$ kg m^{-3}; suspending medium permittivity $\varepsilon_m = 78.5$; and viscosity $\eta = 1.5 \times 10^{-3}$ kg m^{-1} s^{-1}.

The results of the simulation are shown in Figure 6. The solid line indicates the position that

the cells should reach on the electrodes with the above parameters, and the two dotted lines show the distribution that would occur if the cell capacitance is assumed to be constant but the cell radius varies by ±12%. Comparing Figures 5 and 6, the high degree of correlation between the experimental and numerical simulation of particle position is evident.

To demonstrate the potential application of this device for the selective fractionation and retention of cells we simulated the trajectories of the three major cell types found in human blood *viz.* monocytes, T- and B-lymphocytes. The simulation parameters were: electrode potential difference $V_o = 3$ V; chamber width = 8 mm; volume flow rate = 1 ml/hour; applied frequency = 250 kHz; differential density $\Delta\rho = 10$ kg m^{-3} suspending medium conductivity, $\sigma_m = 33$ mS m^{-1}; permittivity $\varepsilon_m = 78$; and viscosity $\eta = 1.5 \times 10^{-3}$ kg m^{-3} s^{-1}. The dielectric properties of the cells were determined from the data of Yang et al. [21], which is reproduced in Table 1.

Figure 7 shows three different plots of simulated particle trajectories calculated for the analytical and the numerical field solutions. Figure 7(a) and (b), curve (i) was calculated with the electrode gap and width both set equal at 40 μm and illustrates the difference that a small discrepancy (13%) in the field gradient can make to the eventual predicted collection position of the particles. All the plots show that the particles are attracted to the electrode array at a position that depends both on the particle size and the dielectric properties of the particle. Comparing the curves (i) and (ii) in Figure 7(b), it can be seen that the calculation is also sensitive to the absolute (precise) value of the electrode gap and width. The simulations shows that not only are particles trapped on the array by positive DEP from the fluid stream, but the device should also be capable of fractionating a mixture of particles into subpopulations with a spacing on the device reflecting the individual dielectric properties of the particles.

Conclusion

A novel dielectrophoretic cell-separation technique has been developed for the separation of rare particles from a fluid stream. A microdevice was constructed from two consecutive arrays of microelectrodes, one to focus the particles into a sheet and the second to separate them using a combination of positive and negative DEP. At a flow rate of 1 ml/hour, experiments showed that THP-1 cells were captured on the electrode array. The experimental results were compared with a 2-D numerical simulation of the particle dynamics. The device is shown to be effective at fractionating subpopulations of cells into different bands along the array.

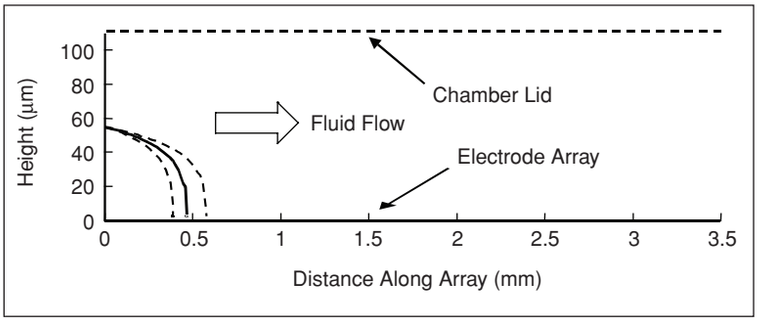

Fig. 6. Numerically simulated trajectories and final position of the THP-1 cells on the electrode array. The conditions were the same as for the experiments with: suspending medium conductivity 26.3 mS m^{-1} (giving a Clausius-Mossotti factor of 0.623 at a frequency of 150 kHz); chamber width = 8 mm; volume flow rate = 1 ml/hour; differential density $\Delta\rho$ =10 kg m^{-3}; suspending medium permittivity $\varepsilon_m = 78.5$; and viscosity $\eta = 1.5 \times 10^{-3}$ kg m^{-3}s^{-1}. The dashed lines represent a ±12% variation in cell radius, giving a spread in final position.

TABLE 1. The dielectric parameters and mean size for the three main cell types found in human blood (taken from Yang et al. (21)).

	Membrane Capacitance (mFm^{-2})	f_{CM} (for σ_m = 33 mS m^{-1})	Radius a (μm)	Cytoplasmic conductivity (Sm^{-1})
Macrophages	$C_m = 15.3$	0.536	4.63	$\sigma_{cyto} = 0.56$
T lymphocytes	$C_m = 10.5$	0.117	3.29	$\sigma_{cyto} = 0.65$
B lymphocytes	$C_m = 12.6$	0.236	3.29	$\sigma_{cyto} = 0.73$

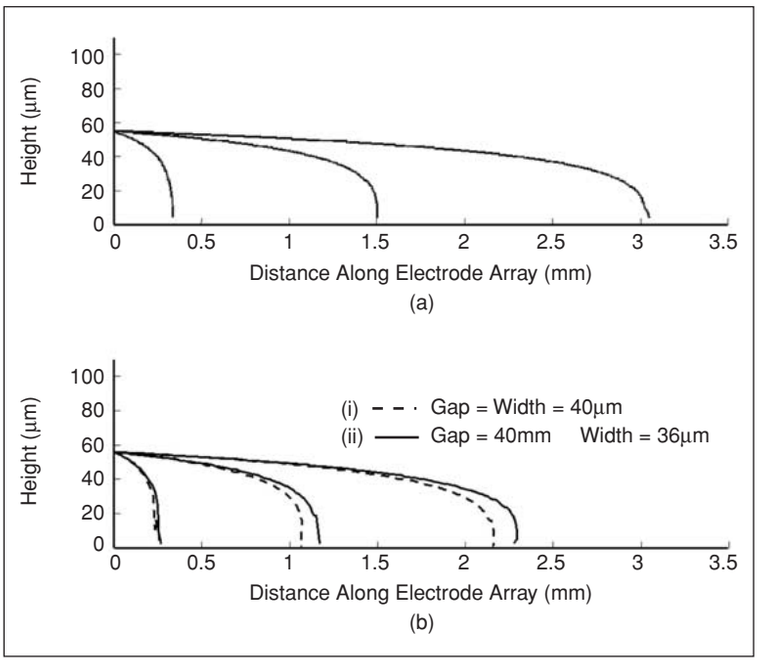

Fig. 7. Plots of simulated particle trajectories calculated for monocytes and T- and B-lymphocytes. (a) is the solution for the analytical Fourier series calculation of the force and (b) the numerical calculation. The two figures show the large difference in trajectories that results from the use of either the analytical or the numerical field solutions. The difference is due to the small discrepancy (13%) in the DEP force. The solid lines in (b), (ii) show the influence of using the correct electrode/gap dimensions in the numerical calculation.

The device is shown to be effective at fractionating subpopulations of cells into different bands along the array.

David Holmes received his B.Eng. degree in electronics and electrical engineering in 1995 and his B.Sc. in neuroscience in 1998 from the University of Glasgow. He was awarded his Ph.D. in Advanced Dielectrophoretic Cell Separation Systems in 2003. He has recently moved from the University of Glasgow to Southampton University, where he is pursuing research on single-cell dielectric spectroscopy. His research interests include the use of electric fields for the manipulation of bioparticles in microsystems and the development of lab-on-a-chip devices for high-throughput rapid analysis and sorting of single biological particles.

Nicolas G. Green graduated from the University of Glasgow with a B.Sc. degree in mathematics and physics in 1994 and a Ph.D. in bioelectronic engineering in 1998. He held a Marie Curie research fellowship at the University of Sevilla in Spain from 1998–2000 and is currently a Royal Academy of Engineering research fellow in the Department of Electronics and Electrical Engineering at the University of Glasgow. His research interests include the use of electric fields for the manipulation of particles and fluids, the separation of mixtures, mixing and pumping, with device applications in micro-analysis systems, and physical chemical and biochemical measurement. His other research interests include theoretical and numerical modelling of these devices and a range of other systems down to atomic-scale modelling of ion conduction. He has recently coauthored a text-book on ac electrokinetics.

Hywel Morgan obtained both his first degree and his Ph.D. at the University of Wales, Bangor, in 1981 and 1985, respectively. He was appointed to a lectureship at the University of Glasgow in 1993, where he established a research program in ac electrokinetics. He was appointed professor of bioelectronics at Glasgow in 2001 and has recently moved to the University of Southampton. In 2001 he was awarded a Royal Society-Leverhulme Senior Research Fellowship. His research interests are concerned with understanding and exploiting the applications of electric fields to biology, particularly in the context of micro and nano-systems. He has developed new bioparticle manipulation and characterization methods and is interested in developing methods for controlling fluids in microsystems through the exploitation of electrohydrodynamic effects. He also has interests in artificial membrane systems and in single molecule imaging. He is a member of the editorial board of the *Journal of Electrostatics*, and recently coauthored a text-book on ac electrokinetics.

Address for Correspondence: Hywel Morgan, School of Electronics and Computer Science, The University of Southhampton, Highfield, Southhampton SO17 1BJ, UK. E-mail: hm@ecs.soton.ac.uk.

References

[1] H.A. Pohl, *Dielectrophoresis*. Cambridge, UK: Cambridge, 1978.
[2] H.A. Pohl and I. Hawk, "Separation of living and dead cells by dielectrophoresis," *Science,* vol. 152, pp. 647–649, 1966.
[3] B.D. Mason and E.G. Hammond, "Dielectrophoretic separation of living cells," *Can. J. Microbiol*., vol. 17, pp. 879–888, 1971.
[4] F.F. Becker, X.-B. Wang, Y. Huang, R. Pethig, J. Vykoukal, and P.R.C. Gascoyne, "Separation of human breast cancer cells from blood by differential dielectric affinity," *Proc. Natl. Acad. Sci. USA*., vol. 92, pp. 860–864, 1995.
[5] G.H. Markx, P.A. Dyda, and R. Pethig, "Dielectrophoretic separation of bacteria using a conductivity gradient," *J. Biotechnology*, vol. 51, pp. 175–180, 1996.
[6] R. Pethig, "Dielectrophoresis: Using inhomogeneous AC electric fields to separate and manipulate cells," *Crit. Rev. Biotechnol.,* vol. 16, pp. 331–348, 1996.
[7] M. Washizu, S. Suzuki, O. Kurosawa, T. Nishizaka, and T. Shinohara, "Molecular dielectrophoresis of biopolymers," *IEEE Trans. Ind. Applicat*., vol. 30, pp. 835–843, 1994.
[8] S. Fiedler, S.G. Shirley, Th. Schnelle, and G. Fuhr, "Dielectrophoretic sorting of particles and cells in a microsystem," *Anal. Chem.*, vol. 70, pp. 1909–1915, 1998.
[9] H. Morgan, M.P. Hughes, and N.G. Green, "Separation of sub-micron bio-particles by dielectrophoresis," *Biophys. J.,* vol. 77, pp. 516–525, 1999.
[10] H. Morgan and N.G. Green, *AC Electrokinetics: Colloids and Nanoparticles.* Herts, UK: Research Studies Press, 2003.
[11] D. Holmes and H. Morgan, "Particle focussing and separation using dielectrophoresis in a microfluidic channel," in *Proc. μTAS 2001*, Monterey, CA, pp. 111–112.
[12] D. Holmes and H. Morgan, "Dielectrophoretic chromatography of cells," in *Proc. μTAS 2002,* Nara, Japan, pp. 829–831.
[13] J. Gimsa, P. Marszalek, U. Loewe, and T.Y. Tsong, "Dielectrophoresis and electrorotation of neurospora slime and murine myeloma cells," *Biophys. J*., vol. 60, pp. 749–760, 1991.
[14] D. Holmes and H. Morgan, "Cell sorting and separation using dielectrophoresis," in *Electrostatic 03* IoP Publishing, UK, 2004,to be published.
[15] T.B. Jones, *Electromechanics of Particles.* Cambridge, UK: Cambridge, 1995.
[16] H. Morgan, A.G. Izquierdo, D.J. Bakewell, N.G. Green, and A. Ramos, "The dielectrophoretic and travelling wave forces for interdigitated electrode arrays: Analytical solution using Fourier series," *J. Phys. D: Appl. Phys*., vol. 34, pp. 1553-1561, 2001.
[17] H. Morgan, A.G. Izquierdo, D.J. Bakewell, N.G. Green, and A. Ramos, "The dielectrophoretic and travelling wave forces for interdigitated electrode arrays: Analytical solution using Fourier series," *Erratum J. Phys. D: Appl. Phys*., vol. 34, pp. 2708, 2001.
[18] N.G. Green, A. Ramos, and H. Morgan, "Numerical solution of the dielectrophoretic and travelling wave forces for interdigitated electrode arrays using the finite element method," *J. Electrostatics,* vol. 56, pp. 235–254, 2002.
[19] X.-J. Wang, X.-B. Wang, F.F. Becker, and P.R.C. Gascoyne, "A theoretical method of electric field analysis for dielectrophoretic electrode arrays using Green's theorem," *J. Phys. D: Appl. Phys.,* vol. 29, pp. 1649–1660, 1996.
[20] M. Garcia and D. Clague, "The 2D electric field above a planar sequence of independent strip electrodes," *J. Phys. D: Appl. Phys.,* vol. 33, pp. 1747–1755, 2000.
[21] J. Yang, Y. Huang, X. Wang, X.-B. Wang, F.F. Becker, and P.R.C. Gascoyne, "Dielectric properties of human leukocyte subpopulations determined by electrorotation as a cell separation criterion," *Biophys. J*., vol. 76, pp. 3307–3314, 1999.